OBSERVATION OF THE ROTATIONAL DOPPLER EFFECT WITH AN OPTICAL-VORTEX ONE-BEAM INTERFEROMETER

A. Ya. BEKSHAEV, I. V. BASISTIY[1], V. V. SLYUSAR[1], M. S. SOSKIN[1], M. V. VASNETSOV[1]

Odesa National University *(Odesa, Ukraine)*,
[1]Institute of Physics, Nat. Acad. Sci. of Ukraine *(Kyiv, Ukraine)*

UDC 532
‰ 2002

Coherent axial superposition of Gaussian and Laguerre – Gaussian LG_0^1 modes produces an optical beam with off-axis optical vortex. The azimuth of the vortex core is a measure of the relative phase shift between the component modes, which allows one to consider such an object as an interferometer with reference and signal waves combined together in a single beam. We have applied the one-beam optical-vortex interferometer for the investigation of optical phenomena associated with the rotational Doppler effect. The frequency difference between the reference and vortex components in a beam reflected from a rotating mirror is manifested by the rotation of the position of the off-axis optical vortex. The origin of the rotational Doppler shift is attributed to the transformational properties of photons with well-defined orbital angular momentum.

Currently, the optics of wave fields possessing phase singularities has become a new chapter in modern optics – singular optics [1]. There are several types of phase singularities in a monochromatic light wave, and the necessary condition for their existence is that the amplitude vanishes at the singularity, resulting in a 'dark thread“ within a wave field, where the phase is indefinite. In analogy with defects in crystals, wavefront dislocations were introduced [2]. A structure of a screw wavefront dislocation looks like a helicoidal surface or a system of $|m|$ helicoids nested on the dislocation axis with a phase distance of $2|m|\pi$ and 2π between neighbour helicoids. The integer m (positive or negative) is the topological charge. An edge phase dislocation is localized perpendicularly to the direction of wave propagation. Nowadays the term 'optical vortex“ (OV) is widely used, reflecting the general feature of phase singularities: phase circulation around the dislocation line. Therefore pure screw dislocation is a core of a 'longitudinal“ OV, and edge dislocation produces a 'transversal“ OV.

Recent researches in singular optics revealed a variety of interesting effects associated with optical vortices. Even in the linear optics frame, the well-known effects of edge diffraction and astigmatic focusing manifest the fascinating phenomena of optical vortices' creation, collision, and reversing of the OV topological sign [3 – 5]. It was predicted recently that an optical beam with helicoidal wavefront attains a frequency shift in the reflection from a rotating mirror [6].

Several experimental schemes were proposed up to now for the detection of the rotational Doppler shift imparted to an OV beam. However, the difficulties in experiment did not allow researchers to perform the detection in the optical region, because a common interference technique demands uncontrollable optical path variations of the compared waves to be much smaller than the wavelength. The only verification of the effect with millimeter waves was reported [7, 8].

The goal of this communication is to report, first to our knowledge, direct optical experiments for the observation of the rotational Doppler effect with helicoidal-wavefront beams. We have elaborated a technique, which allows us to obtain a novel optical scheme suitable for the experimental study of the effect. The basic idea of the experiment is to combine both reference (Gaussian) and signal (OV) beams into a single beam. As was shown earlier [9], coherent coaxial addition of a Gaussian background to the axial (longitudinal) charge-1 OV beam does not destroy the vortex, but shifts its position in the beam cross-section. The OV spatial trajectory coincides no longer with the beam axis and depends on the current phase difference between the constituents.

This given rise to the idea of using such a combined beam as a robust one-beam interferometer, which seems to be an elegant solution to the problem. Any undesirable displacement of optical elements (except rotation) on the beam path will influence equally the phases of the component waves, and the pure rotational contribution can be detected.

1. One-beam Optical Vortex Interferometer

1.1. Concept and Formation

To obtain the necessary superposition of OV and Gaussian beams, different techniques can be used. The disadvantage of separate preparation of the vortex and Gaussian components and their further mixture is evident: the system will be very sensitive to any vibration or slow displacement of the optical elements,

and the beams can possess different waist parameters and therefore Rayleigh ranges. Fortunately, the holographic technique of OV beams creation [10] allows one to avoid easily this obstacle. Both coherent components appear simultaneously in the process of Gaussian beam diffraction by a computer-synthesized grating, whose center is slightly shifted in respect to the readout beam axis.

Let us consider a grating with the transmission function

$$T(\rho, \varphi) = T_0 + T_1(\rho)\cos(K\rho\cos\varphi + M\varphi), \qquad (1)$$

where T_0 is the average transition, $T_1(\rho)$ is the contrast, K is the grating periodicity parameter, integer M is the strength of the imprinted phase singularity. Taking into account that $\rho\cos\varphi = x$, the field behind the grating illuminated by a plane wave can be expressed as the sum of zeroth and plus/minus first diffraction order:

$$E = T_0\exp(ikz) + T_1(\rho)[\exp(ikz + iKx + iM\varphi) +$$

$$+ \exp(ikz - iKx - iM\varphi)]/2. \qquad (2)$$

The first order beam with the phase term $kz + M\varphi$ possesses a negative OV for positive M (left helicoid of the wavefront), the minus-first order carries a positive OV.

If we accept the linear dependence of the contrast $T_1(\rho) \sim \rho/R$, where R is the grating radius, then, for the singularity strength $M = 1$, the readout Gaussian beam with the waist at the plane of the grating and the spot size $w_0 \ll R$ will produce the first diffracted order exactly as the Laguerre – Gaussian mode LG_0^1:

$$E_1 \sim \frac{\rho}{R}\exp\left(-\frac{\rho^2}{w_0^2} + i\varphi\right) \qquad (3)$$

or, in Cartesian coordinates, equivalently

$$E_1 \sim \frac{x + iy}{R}\exp\left(-\frac{x^2 + y^2}{w_0^2}\right). \qquad (4)$$

In the situation where the grating center is slightly shifted from the readout beam center, say by a distance $x_0 \ll R$, the diffracted order field becomes

$$E_1 \sim \frac{x + x_0 + iy}{R}\exp\left(-\frac{x^2 + y^2}{w_0^2}\right) =$$

$$= \frac{x_0 + \rho\exp(i\varphi)}{R}\exp\left(-\frac{\rho^2}{w_0^2}\right), \qquad (5)$$

which is a coaxial superposition of the Gaussian component $(x_0/R)\exp(-\rho^2/w_0^2)$ and LG_0^1 mode.

The grating shown in Fig. 1,*a* possesses linear modulation of the fringes contrast and is suitable for the pure LG_0^1 mode creation as well as for the mode superposition necessary for the one-beam interferometer operation (Fig. 1,*b*). However, if the displacement or the beam spot is comparable with the grating radius, the boundary diffraction will destroy the mode structure.

Note that, generally, in the one-beam interferometer configuration, the superposition of a higher LG_0^l mode with the Gaussian component can also be realized. The corresponding field distribution at the common waist of the modes can be expressed in the form

$$E_1 \sim [E_G + E_{LG}\rho^{|l|}\exp(il\varphi)]\exp(-\rho^2/w_0^2), \qquad (6)$$

where E_G is the amplitude of the Gaussian component, E_{LG} is the amplitude of the Laguerre – Gaussian component LG_0^l, carrying an optical vortex with charge l.

1.2. Principles of Operation

Like other interferometric instruments, the one-beam interferometer serves for revealing the phase or frequency difference between two coherent optical fields – namely, between the Gaussian and LG_0^1 modes composing beam (5). This beam has the transverse intensity distribution with a dark spot (OV core) at the point when the sum amplitude gets zero value, i.e. at $\rho_0 = x_0$, $\varphi_0 = \pi$ in polar coordinates (see Fig. 2,*a*). The off-axis OV radial position is proportional to the grating displacement (contribution of the Gaussian component) and can be easily controlled.

Let the LG_0^1 component obtain a phase shift δ so that, instead of (5), we have

$$E_1(\delta) \sim \frac{x_0 + \rho\exp[i(\delta + \varphi)]}{R}\exp\left(-\frac{\rho^2}{w_0^2}\right). \qquad (7)$$

This distribution differs from expression (5) only by replacing $\varphi \to \varphi + \delta$; consequently, the vortex moves to the point $\rho_0 = x_0$, $\varphi_0 = \pi - \delta$, and the dark spot turns clockwise (when seeing against the beam propagation) by the angle δ (Fig. 2,*b*). The same rotation happens if we correspondingly change the

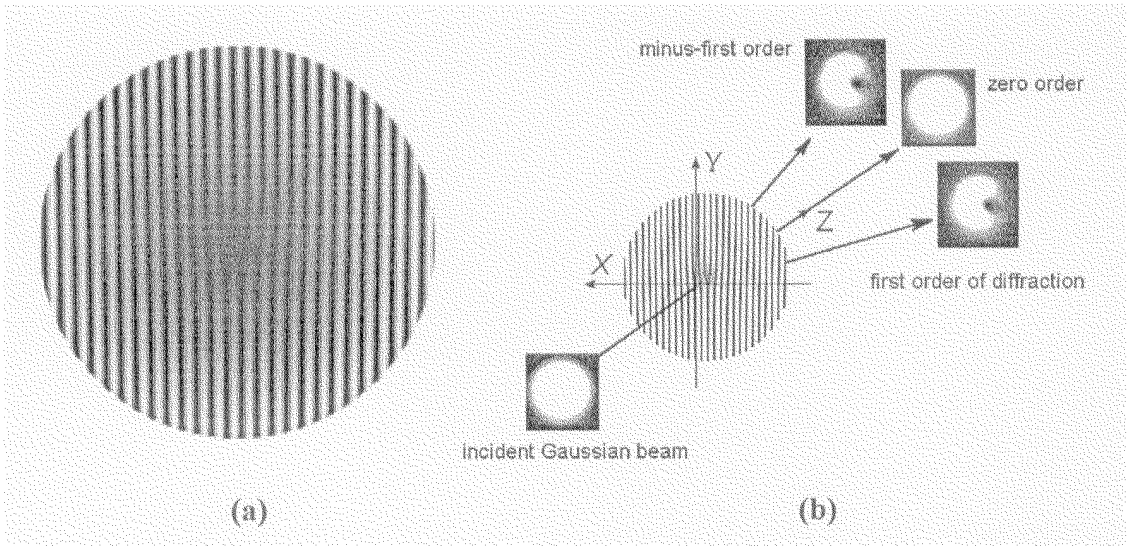

Fig. 1. *a* – example of a computer-synthesized hologram suitable for OV beam production in the first diffracted order: grating with linear modulation of the fringes contrast, developed for the LG_0^1 mode creation, $M = 1$. *b* – schematical representation of the diffraction by the grating displaced with respect to the readout Gaussian beam. Diffracted beams in the near field are shown

phase of the Gaussian component, e.g. by grating displacement $x = x_0$, $y = -x_0 \operatorname{tg}(\delta)$. This nontrivial property opens the possibility to move the optical vortex zero-amplitude center on the nano-scale by proper displacement of a computer-generated grating, which can find various applications.

In case of opposite vortex sign (i.e., when φ is replaced by $-\varphi$ in (5), (6) and the consecutive relations), the same frequency deviation will cause the dark spot to rotate in the opposite direction.

Therefore, any phase shift between the LG_0^1 and Gaussian components can be seen by the dark spot turn within a beam. In particular, this fact can be utilized for expressive demonstration of the Gouy phase variations of propagating beams [9]. Since both components propagate in the free space with identical laws of diffraction spread-out, i.e. with equal Rayleigh ranges and spherical components of the wavefront curvature, the only difference appears in the Gouy phase shift, which amounts to $\operatorname{arctg}(z/z_R)$ for the Gaussian component and $2\operatorname{arctg}(z/z_R)$ for the 'doughnut" LG_0^1 mode. The initial relative phase shift between the components is determined by the direction of the grating displacement. On a way from the grating to the far field, the OV azimuth will change due to the difference of the Gouy phase shifts: the dark spot will make a turn clockwise by 90° for a negative vortex and – 90° for a positive one (looking along the beam propagation). This is a simplest manifestation of the one-beam interferometer operation.

The property of the off-axis OV azimuth to be sensitive to the phase shift between the combined beam components is equally helpful for the study of the rotational Doppler effect. Let us consider the reflection of the combined beam from a reflector, rotating around the beam axis. In this case, the frequency of the Gaussian beam does not change while the frequency ω of the LG vortex mode undergoes a certain deviation $\omega \to \omega + \Delta\omega$, [5] which leads to the time-dependent phase shift $\delta = -\Delta\omega t$ (recall that the time dependence of the optical field is described by the factor $\exp(-i\omega t)$). Of course, this phase shift will result in the dark spot rotation. According to the above consideration, the absolute value of the dark spot azimuth turn will amount to δ, i.e. the dark spot will continuously rotate with the angular velocity

$$d\varphi_0/dt = -d\delta/dt = \Delta\omega. \qquad (8)$$

In other words, the dark spot rotation can serve as an exact measure of the LG mode phase and frequency deviation with respect to the Gaussian component (reference).

Now suppose that an optical detector collects the light energy coming on a certain part of the area shown in Fig. 2. Due to the rotation of the intensity distribution in the beam cross-section, the detector signal will change periodically with the rotation frequency $\Delta\omega$. This means that the one-beam interferometer can show the time behavior similar to that used for the measurement of the rotational Doppler shift in the two-beam scheme [7].

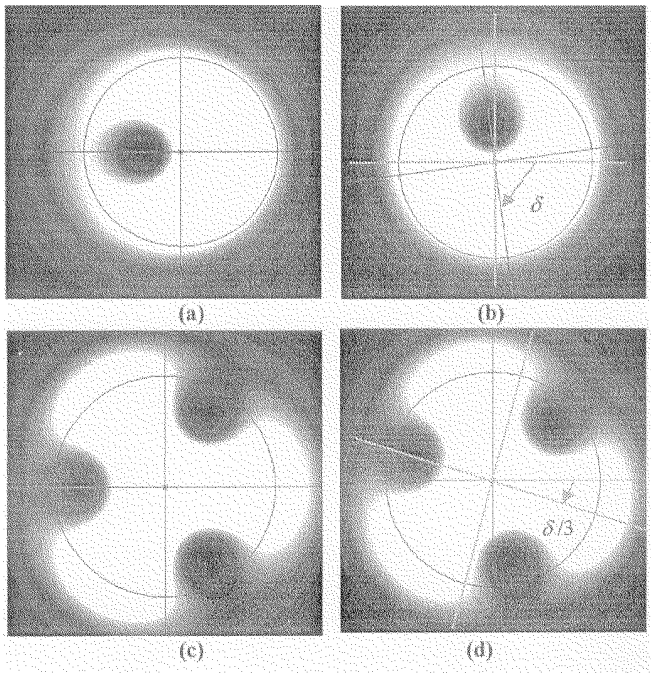

Fig. 2. Views of the beam spot in the one-beam interferometer for zero phase difference between the Gaussian and vortex components (left column) and for phase difference δ (right column). The OV charge in the vortex component equals 1 (*a*, *b*) and 3 (*c*, *d*). The *Z*-axis is directed towards the reader

Advert also to the situation when the beam has the more complicated form (6). Then the beam cross-section contains l dark 'holes“ positioned at the points $\rho_0 = x_0$, $\varphi_0 = [(2n - 1)\pi - \delta]/|l|$ $(n = 1, 2` \ldots |l|)$. Therefore, with the same frequency difference, the pattern of LG_0^l mode ¯ Gaussian beam superposition will rotate $|l|$ times slower than the simplest combination (5) (see Fig. 2,*c*, *d*). Nevertheless, the frequency of the detector signal time variations still exactly equals to the vortex component frequency deviation $\Delta\omega$. Further in Section 3, we shall show that the observable frequency shift is proportional to l in the case of the rotational Doppler effect, so the beam rotation does not depend on l and the frequency of the detector beatings is expected to be $|l|$ times higher for a multiple charge OV beam.

2. Experiment

The gratings possessing the charge-1 phase singularity were produced with a usual technique of printing the pattern on a paper and reducing the size by photocopying [9]. In contrast to usual binary computer-synthesized gratings, we have generated a gray-scale grating with linear modulation of fringes contrast, according to the transmission function $T_1(\rho) \sim \rho/R$ (Fig. 1,*a*). With the radius of the grating on a photofilm $R \approx 2.5$ mm and the spot radius of the focused He¯Ne laser beam $w_0 \approx 0.25$ mm, the necessary condition $w_0 << R$ was satisfied. In the first diffraction order, we obtain a 'pure“ LG_0^1 mode, which does not change the transversal shape along the propagation path. Small displacement of the grating center (less than the beam spot size) with respect to the beam axis resulted in off-axis OV in the diffracted beam, thus providing the necessary superposition of the Gaussian and OV components. We have chosen the first (right) diffracted order, which possesses the left helicoid of the wavefront (negative OV charge) for the vertical direction of the grating 'fork“.

We have used several experimental schemes to observe the influence of the reflected beam rotation on the phase and frequency shift between the Gaussian and vortex components. The one most suitable for precise measurements is shown in Fig. 3. The main purpose of this scheme is to produce the beam rotation, which is achieved by a 90° glass prism rotating around the incident beam axis. The incident beam experiences two total internal reflections within the prism, and the output beam leaves the prism just in the opposite direction with respect to the incident beam. Each reflection reverses the sign of the OV topological charge, thus the retro-reflected beam has the same OV sign as the incident one. (We note that a simple retro-reflection by a mirror reverses both the direction of the beam and the OV sign).

The rest of the system serves for visualizing and measuring the rotational phase shift: the beam-splitter partially reflects the retro-reflected beam, which is afterwards focused by the lens to the focal spot, where the CCD camera picks up the off-axis dark spot image.

The experimentally obtained pictures are shown in Fig. 4. The OV beam was prepared with a horizantal displacement of the grating, and therefore the azimuth of the dark spot amounted to $\varphi_0 = \pi$ in the near field. To eliminate the influence of the inherent dark spot rotation in the near field, the distance from the grating to the rotator was taken several Rayleigh ranges. Under these conditions, the input beam has the dark spot oriented vertically. Due to the presence of the focusing lens in the scheme, the observed dark spot on a screen was oriented again horizontally for the angle $\theta = 0$ of the prism orientation. The prism rotation produces the off-axis vortex rotation, with the twofold rate relatively to the prism motion. The left column shows the interferometer output for the selected angles θ from zero to 90°. The resulting angle of the OV clockwise rotation amounts to 180°. The right collumn shows the pictures corresponding to the prism rotation from zero to − 90°. The counterclockwise OV rotation also reaches the angle − 180°.

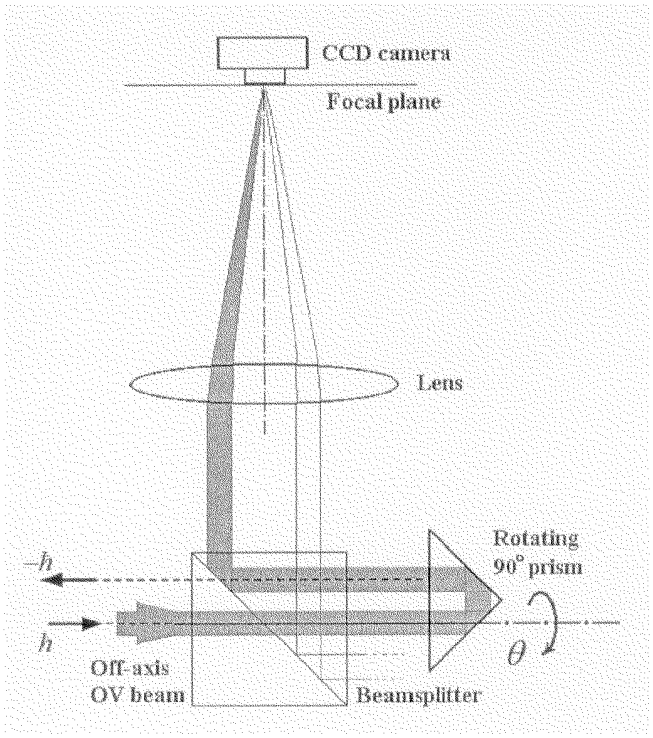

Fig. 3. Back-reflection scheme with the 90° prism, rotating around the axis of the incident beam. The retro-reflected beam is directed by a beam-splitter to the focusing spherical lens. Independently on the angle of the prism orientation, the beam will come to the same spot in the focal plane of the lens, where the CCD camera is placed. The beam path for the angle $\theta = 0$ (shaded area) is shown, the beam path for the angle $\theta = 180°$ is also shown

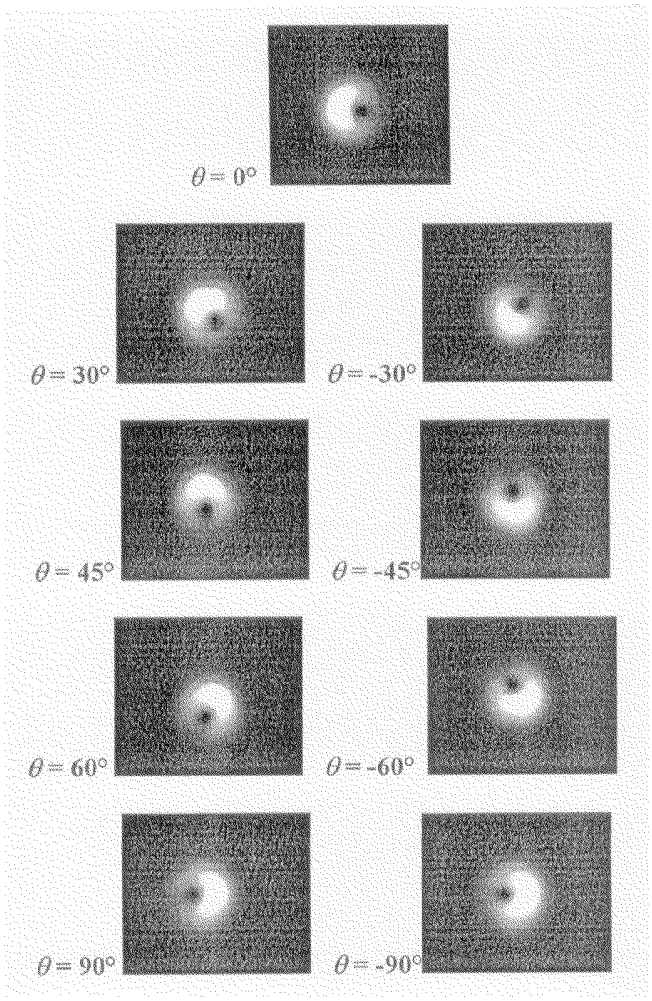

Fig. 4. Experimental observation of the off-axis OV rotation in the one-beam interferometer (scheme shown in Fig. 3)

We note that the use of a single mirror rotating about the beam axis also produces the rotation of the dark spot in the reflected beam, when the beam is reflected 'forward“, i.e. the angle of incidence exceeds 45°. In the opposite case, the 'backward“ reflection does not produce the image rotation. Due to the insensitivity of the one-beam interferometer to any vibrations, the effect is observable even while holding the mirror in a hand.

3. Discussion and Conclusion

To calculate the corresponding frequency deviation of the vortex component, we can use the energy approach and mechanical analogy [6, 7]. It is known [1] that any OV beam carries the orbital angular momentum (OAM). Let us represent the vortex component (left helicoid of the wavefront) as a flux of photons every carrying the energy $\varepsilon = \hbar\omega$ and the OAM $\hbar$. In the laboratory coordinate system, each retro-reflected photon carries OAM $-\hbar$, i.e. the OAM quantity $2\hbar$ is imparted to the prism during an act of a photon retro-reflection. The beam rotation associated with this angular momentum has the same direction as the prism rotation (see Fig. 3) so that, in this interaction, the photon transfers a part of its energy to the prism. The prism rotation with the angular velocity $d\theta/dt = \Omega$ changes the photon energy by $\Delta\varepsilon = -2\hbar\Omega = \hbar\Delta\omega$, whence the output beam frequency deviation follows as $\Delta\omega = -2\Omega$. Comparing this to Eq. (8), we make a conclusion that the output picture in the system of Fig. 3 will rotate with the angular velocity 2Ω.

For a multiple charge left-helicoidal OV, every photon carries the OAM $l\hbar$ and the analogous discourse gives the frequency shift of the output vortex component $\Delta\omega = -2l\Omega$. Due to the conclusive remark of Section 2.2, this means that the angular velocity of the pattern of several ($|l|$) dark spots does not depend on l, but results in measured intensity beatings the $|l|$-times higher frequency $2l\Omega$.

Rather surprisingly, the direction of the rotation does not depend on the sign of the OV. Reversing the OV sign in the incident beam (right helicoidal wavefront) will reverse the corresponding frequency shift to $\Delta\omega = +2\Omega$. Since both the signs of the input OV and frequency shift are reversed, the direction of the dark spot rotation remains unaffected, in accordance with the note in Section 1.2.

The experimental results of the off-axis OV behavior are in absolute agreement with the theoretical expectations based on the direct consideration of energy exchange between the vortex beam and optical elements. This is not very surprising; one may notice that the same behavior of the off-axis OV beam can also be explained by a simple geometric optics reasoning.

The essence of the rotational Doppler effect consists in the transformation of the coordinate frame. Rotation of the reflector results in the rotation of the image (dark spot in our case), as well as the frame, thus producing the phase change of the OV beam in the laboratory coordinate system, while the Gaussian component does not change the phase.

On the first stage of the above-described experiment, we had to 'prepare“ the rotational phase or frequency shift, for which purpose the rotating prism imparted the necessary rotary motion to the beam. On the second state (detection), this very motion was used for the rotational Doppler shift revelation and measurement. In other words, the image (dark spot) rotation and the phase shift of the vortex component are equally the cause and the effect for each other. This is a consequence of the deep interconnection between the spatial and phase properties of vortex LG modes [6], which makes the one-beam interferometer with Gaussian and vortex beam superposition to be a unique instrument for rotational Doppler effect investigations. In this sense, the use of a one-beam interferometer makes the rotational Doppler shift quite obvious and, simultaneously, makes apparent its intrinsic source lying in the transformational properties of photons with well-defined OAM [6, 7].

There is also a variety of possible other experimental verifications of the effect. Among them, a simple scheme of the rotation of the grating itself attracts the attention and was just realized by us [11].

1. *Soskin M.S., Vasnetsov M.V.*//Prog. in Optics. **42**, Ch. 4, 219 (2001).
2. *Nye J.F., Berry M.V.*//Proc. Royal Society of London A. **336**, 165 (1974).
3. *Vasnetsov M.V., Marienko I.G., Soskin M.S.*//JETP Lett. **71**, 192 (2000).
4. *Molina-Terriza G., Recolons J., Torres J.P., Torner L.*//Phys. Rev. Lett. **87**, 023902 (2001).
5. *Bekshaev A.Ya., Vasnetsov M.V., Denisenko V.G., Soskin M.S.* //JETP Lett. **75**, 155 (2002).
6. *Bekshaev A.Ya.*//Optics and Spectroscopy. **88**, 993 (2000).
7. *Courtial J., Dholakia K., Robertson D.A. et al.*//Phys. Rev. Lett. **80**, 3217 (1998).
8. *Courtial J., Robertson D.A., Dholakia K. et al.*//Ibid. 4828 (1998).
9. *Basistiy I.V., Bazhenov V.Yu., Soskin M.S., Vasnetsov M.V.*//Opt. Communs. **103**, 422 (1993).
10. *Bazhenov V.Yu., Vasnetsov M.V., Soskin M.S.*//JETP Lett. **52**, 429 (1990).
11. *Basistiy I.V., Bekshaev A.Ya., Vasnetsov M.V., Slyusar V.V., Soskin M.S.*//JETP Lett. **78**, 556 (2002) (in Russian).

Received 24.05.02